

International Engineering Research Journal

Design and Optimization of Scale down Flow Model for Wire Plate Electrostatic Precipitator using Gas Distribution Screen

Supriya kamble, manish Attal, and Vasantha Ramaswamy

Dept. Of Mechanical Engineering, sinhgad college of engineering, Savitribai Phule Pune University, Pune, Vadgaon, India
Assistant Professor, Sinhgad College of engineering, Savitribai Phule Pune University, Pune, Vadgaon, India
Director, Aprameya Associate. Aundh, Pune India

Abstract:

Electrostatic Precipitators (ESP) are industrially used control devices to capture fine particles for reducing exhaust emission. Performance of electrostatic precipitator is affected by its complex flow distribution arising due to its complex geometry. Gas distribution screens are used as efficient distributing member in fluid flow control. The present study aims at simulation of flow behavior within electrostatic precipitator and finding standard porosity pattern, scale down actual model of ESP and validate scale down process numerically using computational fluid dynamics (CFD). Scale down model to 1/10th by considering geometrical, kinematical, dynamic similarity between actual and scale down will be carried out. Optimized scale down flow modelled is use to predict performance of ESP at design stage. Gas distribution screen with both uniform porosity and variable porosity are considered for the purpose of optimization

Keywords: electrostatic precipitator, computational fluid dynamics, flow pattern, porosity.

1. Introduction

Particulate matter emission is one of the major air pollution problems of coal fired power plants. Fine particles are smaller fraction by weight of the total suspended particle. ESP is widely used as efficient reliable particulate emission control device in industries and power plants. Gas velocity characteristics inside the ESP plays important role in performance of ESP. For achieving better collection efficiency at collecting plates in field, the flow inside the treatment zone of electrostatic precipitator should be uniformly distributed and moving slowly. When flow enters in the diffuser velocity reduce up to one tenth of inlet velocity. When flow enters the diffuser at inlet it faces sudden pressure drop that causes flow separation due to which flow concentrate in localized area and result in non-uniform flow distribution in field. The solution to this problem is to use the gas distribution screen for controlling flow at upstream of treatment zone. For controlling the flow one porosity distribution screens at outlet and three porosity distribution screens at inlet are used. High velocity as well as low velocity regions are present in ESP uniform gas distribution screens are unable to distribute flow uniformly. Non uniform porosity distribution screen gives best result by keeping high resistance or low opening at high velocity region and low resistance or high opening at low velocity region the flow can be distributed uniformly.

The objective of this paper is to describe a detail numerical method and an approach adopted to forecast the flow pattern inside a full scale ESP and Scale down of full scale model

2 Geometry of ESP

ESP consist of two fields. Each field contains 29 collecting plates and 28 Passages with 300 spacing in between. Each plate thickness 10mm and width and length. Esp. consist of four hopper for collecting dust. It has single inlet and outlet duct. Three perforated plate are located at inlet and one at outlet for efficient distribution of gas.

2.1 modelling:

Cad drawing with dimensions received from client is studied and as per client specification 3D model is drawn in CATIA and Geometry drawn in CATIA then import in hyper mesh for discretization. Fig.1 shows model of ESP drawn by using CATIA.

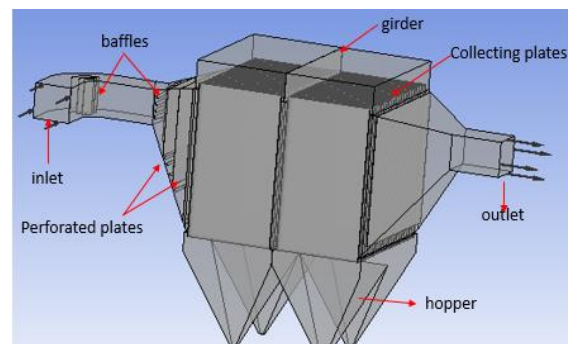


Fig 1 Typical 3D ESP geometry

2.2 Meshing:

Meshing done in HYPERMESH-14. Discretization of fluid domain into small cells to form a volume grid and set up the suitable boundary conditions. HYPERMESH is popular software use for mesh generation. Ability to generate high quality mesh quickly is one of HYPERMESH's core competencies. Structural meshing gives accurate result compare to unstructured mesh. Structural mesh takes time to generate compare to unstructured mesh. Structural mesh is generated by dividing model into number of parts and 3D mesh generate. Computational meshes varies from 10, 00,000 to 22,00,000 depending on the size. Define boundaries. Fig 2 shows hexahedral mesh in HYPRMESH.

Table 1 Result deviation due to change in mesh count

Mesh count (in lakhs)	% deviation
10-15	10 %
15-20	6 %
20-22	2%

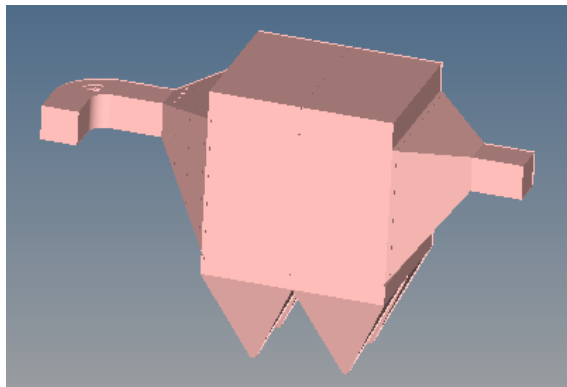


Fig 2 computational mesh of ESP

3. Simulation:

Meshing file from HYPRMESH import in ANSYS CFX. Standard K-ε model is used for turbulence modelling which widely use in industries for internal flow.

Governing equations:

Numerical computation of all fluid flow CFX solves conservation of mass, momentum and transport equations (if the flow is turbulent) for fluid in given flow geometry. The basis of modeling of an incompressible Newtonian fluid flow module is the use of the conservation of mass equations.

$$\frac{\partial \rho}{\partial t} + \nabla \cdot (\rho v) = 0 \quad (1)$$

And the Navier-Stokes equation in x, y and z direction.

$$\frac{\partial (\rho u)}{\partial t} + \nabla \cdot (\rho u) = -\frac{d\rho}{dx} + \nabla \cdot (\nabla u) + \rho g_x \quad (2)$$

$$\frac{\partial (\rho v)}{\partial t} + \nabla \cdot (\rho v) = -\frac{d\rho}{dy} + \nabla \cdot (\nabla v) + \rho g_y \quad (3)$$

$$\frac{\partial (\rho w)}{\partial t} + \nabla \cdot (\rho w) = -\frac{d\rho}{dz} + \nabla \cdot (\nabla w) + \rho g_z \quad (4)$$

For the turbulent flow in ESPs, accurate description of turbulence model is the key to the success of CFD. To model the turbulent flow in an ESP, there are a number of turbulence models available. Mixing length model is basic model in turbulence model. If the convection and diffusion of turbulence properties are neglected it is possible to exhibit the influence of turbulence on flow in terms of the mixing length. If convection and diffusion are not negligible-as is the case for example in recirculating flows equation of mixing length is no longer workable. It is a two equation model which gives a general description of turbulence by means of two transport equations. The first transported variable K determines the energy in the turbulence and is called turbulent kinetic energy (k). The second transported variable epsilon is the turbulent dissipation which determines the rate of dissipation of the turbulent kinetic energy.

The turbulence kinetic energy, k, and its rate of dissipation, ε, are obtained from the following transport equations.

$$\frac{\partial (\rho k)}{\partial t} + \frac{\partial (\rho k u_j)}{\partial x_j} = \frac{\partial}{\partial x_j} \left[\left(\nabla + \frac{\nabla_t}{\sigma_k} \right) \frac{\partial k}{\partial x_j} \right] + G_k + G_b - \rho \epsilon - Y_M + S_K \quad (5)$$

$$\frac{\partial (\rho \epsilon)}{\partial t} + \frac{\partial (\rho \epsilon u_j)}{\partial x_j} = \frac{\partial}{\partial x_j} \left[\left(\nabla + \frac{\nabla_t}{\sigma_\epsilon} \right) \frac{\partial \epsilon}{\partial x_j} \right] + \rho C_1 S_\epsilon - \rho C_2 \frac{\epsilon^2}{k + \sqrt{v \epsilon}} + C_{1\epsilon} \frac{\epsilon}{k} C_{3\epsilon} G_b + S_\epsilon \quad (6)$$

Where

$$C_1 = \max \left[0.43 \frac{\eta}{\eta + 5} \right], \quad \eta = S \frac{k}{\epsilon}, \quad S = \sqrt{2 S_{ij} S_{ij}} \quad (7)$$

G_k : Generation of turbulence kinetic energy due to the mean velocity gradients

G_b : Generation of turbulence kinetic energy due to buoyancy

Y_M : Contribution of the fluctuating dilatation in compressible turbulence to the overall dissipation rate

C_1 & C_2 : constants.

Σk and σ_ϵ : turbulent Prandtl numbers for k and ε, respectively.

S_K and S_ϵ : user defined source terms. The model constants C_1, C_2, σ_k and σ_ϵ have the following default values. $C_1 = 1.44, C_2 = 1.9, \sigma_k = 1.0, \sigma_\epsilon = 1.2$

3.1 Model consideration:

Main purpose of the project is to analyze the gas flow distribution and pressure loss. The effect of particle concentration in gas flow and its distribution in the ESP is not considered in the simulation.

Flow is considered as steady state, incompressible and isothermal with fluid properties at given operating temperature. (Vacuum pressure).

1) Atmospheric air at 25 degree C is considered as working fluid.

2) Steady state conditions is consider for.

3) Single phase analysis.

4) Flow rate is given as $60 \text{ m}^3/\text{s}$.

5) Out pressure is 82mm of water column.

Boundary conditions:

Inlet – velocity inlet.

Outlet – pressure outlet.

Gas distribution screen –porous media model

Convergent, divergent sections, casing, hopper, girders, hopper baffle, collecting plates

Flow rate of ESP given in CAD sheet and inlet area can be calculated using inlet duct dimensions. Velocity calculate by dividing flow rate by its cross section area. This calculated velocity assigned to inlet. Pressure at an outlet of ESP is 82 mm of water column given by client. So pressure boundary condition assign to outlet. Gas distribution screens has porosity consist of circular holes with very small diameter. Meshing of such small holes is complex because it is difficult to capture such thousands of small holes. Mesh count goes very high if we do this mesh and computational efforts increases. To avoid high mesh count and for saving time, porous media model is used for GD screen.

3.2. Perforated plate modelling.

Three perforated plate at inlet and one perforated plate are used in ESP for distributing the gas flow uniformly in the diffuser. The thickness of perforated plate is 10mm in actual and asper opening of perforated plate number of holes are punched on screen. Diameter of hole is remain same in perforated plate its porosity is varied by varying the pitch. As pitch is decrease the distance between the holes is decreased and percentage open area increases and vice versa. There are different openings used for GD screens such as 30%, 40%, 45%, 50%, 35% and 60%. It is very difficult to control the flow with uniform porosity the variable porosity of perforated plate is effective to achieve uniform flow distribution inside the ESP. there is non uniform flow concentration along the screen. Porous media of finite thickness with permeability over which resistance coefficient C2 is calculated by equation of Van Winkle, show how porous media inputs can be calculated for pressure loss through a perforated plate with square-edged holes.

$$\frac{\Delta p}{\Delta x} = \left(\frac{1}{2}\rho v^2\right) \frac{1}{C^2} \frac{\left(\frac{A_p}{A_f}\right)^2 - 1}{t} \quad (8)$$

Where,

$$C_2 = \frac{1}{C^2} \frac{\left(\frac{A_p}{A_f}\right)^2 - 1}{t} \quad (9)$$

A_f = free area or total area of hole

A_p = area of plate

C = coefficient that has been tabulated for various Reynold number range and various D/t

D/t = ratio of hole diameter to plate thickness.

for D/t > 1.6 and for Re > 4000 the coefficient C takes a value of approximately 0.98

Table 2 resistance coefficient values for percentage opening

sr.no	%opening	resistance coefficient value(C2)m ⁻¹
1	30	1052.8
2	40	546.64
3	50	312.36
4	60	185.1
5	45	410
6	35	746

3.3 Criteria of acceptance:

All ESP's should follow Standards set by the Institute of Clean Air Companies (ICAC) for attaining maximum efficiency through uniform flow distribution. The velocity inside treatment zone of ESP a minimum of 85% of the velocities not more than 1.15 times the average velocity and 99% of the velocities not more than 1.40 times the average velocity. Average velocity is mean of all velocity measurements made at a given face of the precipitator. as per ICAC standards all this velocities should be measured near inlet and outlet of the precipitator field, this ESP consist of two fields. Velocity measurements made at first field inlet, second field inlet, and second field outlet.

RMS value.

Percent RMS deviation of the measured/modelled velocity versus the average velocity. The percent RMS is calculated by the following formula:

$$\%RMS = \frac{100}{V_{avg}} \sqrt{\frac{\sum(V_i - V_{avg})^2}{\sum(i-1)}} \quad (10)$$

Where,

v_i = velocity at select grid point

v_{avg} = average velocity over entire plane

The goal in industry is to achieve a Percent RMS of less than 20% at the inlet and outlet planes of field.

4. Discussion and result

Wide angle diffuser has larger angle and area ratio than common diffuser. When flow enters the diffuser inlet it faces the sudden pressure drop because of this sudden pressure drop, flow separation takes place in diffuser. Due to flow separation in diffuser pressure rise ability of diffuser decrease and pressure loss increases. When flow enter in diffuser area increase gradually because of that kinetic energy convert into pressure energy. After passing flow through first perforated plate flow get distributed to wall of diffuser and central low velocity region is created. After passing flow through first perforated plate centrally accumulated flow in diffuser get distributed symmetrically and low velocity region created centrally.

Flow consist of as dust particle. When flow impinge on perforated screen some dust particle are stick to the screen and after some time due to gravitational force they fall down and collected at the bottom of diffuser. For removing this dust 100 mm opening is kept at the bottom of all gas distribution screen. Because of this opening at bottom of perforated plate flow flows

through that opening and slip down directly in hopper and cause recirculation of flow
 With given boundary condition and all gas distribution screen opening is 50%, so simulation is carried out, following result are occurred.

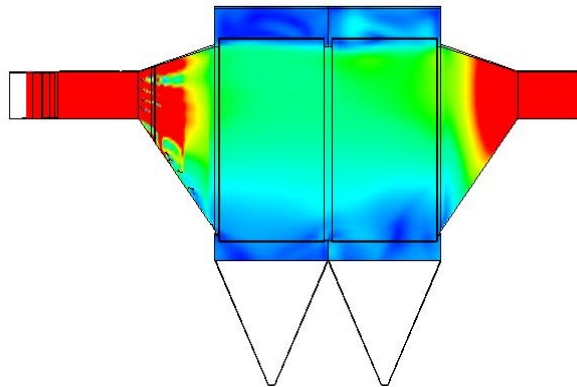


Fig. 3 Velocity contour plot

From above fig 3 of velocity contour shows that maximum gas flow passes through upper area of electroplate with high velocity, moderate velocity at middle section and less velocity zone created bottom section of collecting plates of first field it means non uniform flow distribution occur in treatment zone.

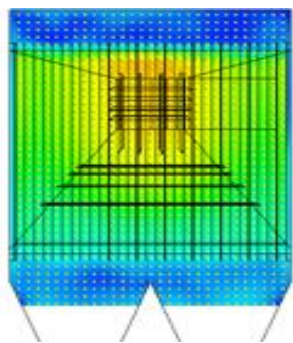


Fig 4 Velocity contour at second field inlet of ESP before modification

Table 3 Initial flow Result at inlet plane

AVERAGE VELOCITY	0.8560
R.M.S	28%
1.15 X AVG VEL	1.198401
1.4 X AVG VEL	0.984401
POINTS BELOW 1.15 X AVG VEL	271
POINTS BELOW 1.4 X AVG VEL	338
TOTAL POINTS	377
% POINTS BELOW 1.15 X AVG	72
% POINTS BELOW 1.4 X AVG VEL	85

Fig 4 velocity counters at inlet of second field it shows less flow at lower and maximum flow accumulated at

upper middle section. As per table result of velocity contour of first field outlet RMS and % Average velocities are not meet as per ICAC standards. Percentage opening kept for first inlet gas distribution screen is shown in fig. before and after modification.

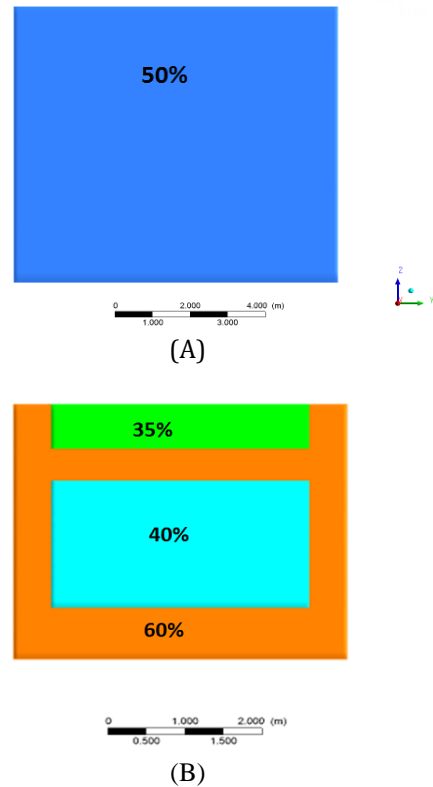
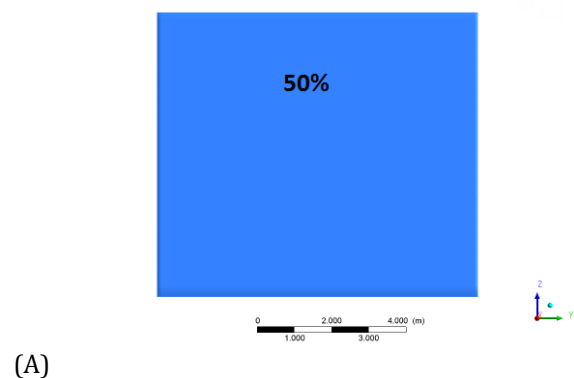
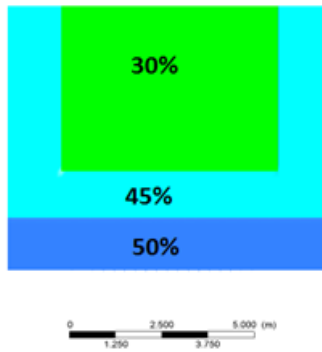


Fig 5 First gas distribution screen opening percentage. (A) Before optimization. (B) After optimization.

Velocity profile along the third gas distribution screen is uniform it not need to change. But for gas distribution screen first and second it need to be optimized for achieving uniform flow. Along the first distribution screen high velocity observe at upper and middle section for restricting flow at upper side kept 35% and middle side kept 40% opening in between upper and middle zone due to baffle void section is created, and also at bottom due to improper distribution flow void zone create because of that in those region kept 60% opening.





(B)

Fig 6 Forth gas distribution screen opening percentage. (A) Before optimization. (B) After optimization.

Fig shows convergent nozzle gas distribution screen percentage opening modification. At upper central zone of GD screen maximum flow accumulated and low velocity region present at bottom zone so that for uniform flow distribution in second field forth GD screen modifies as 30%, 45%, 50% opening are kept for uniform flow.

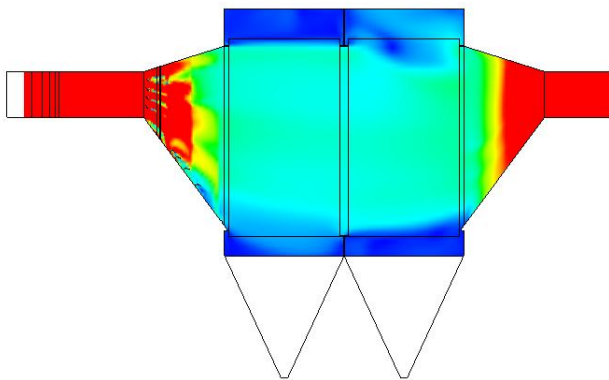


Fig 7 Optimized Velocity contour plot

Fig 7 shows velocity contour after gas distribution screen modifications. As we can see from Fig 7 that flow is uniformly distributed on mid-section of ESP. High velocity region at the upper of casing is removed. Fig. shows velocity contour at end of first field. High velocity patches observed at top and low velocity region at bottom of casing is removed.

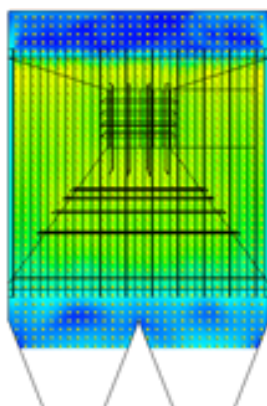


Fig 8 Velocity contour at second field inlet of ESP after modification

Table 4 flow result after optimization

AVERAGE VELOCITY	0.9326
R.M.S	15.72
1.15 X AVG VEL	1.072537
1.4 X AVG VEL	1.305698
POINTS BELOW 1.15 X AVG VEL	341
POINTS BELOW 1.4 X AVG VEL	377
TOTAL POINTS	377
% POINTS BELOW 1.15 X AVG VEL	90
% POINTS BELOW 1.4 X AVG VEL	100

Velocity reading at 377 number of points are taken at the end of first field to validate the data. It is observed that velocity readings at the end of first field follows ICAC criteria shown in table.

Perforated plate openings are validate by experimentally, numerically and analytically. Numerically and analytically is validated by comparing pressure drop across perforated plate. Validation through experimentally is in progress.

5 Scale Down:

Physical model method have been utilizing for understand fluid flow characteristics. Physical models are basically laboratory performance testing of an actual model. An ESP is typically modelled in 1/10th. These models are constructed from clear acrylic to clear flow visualization. Strength of Acrylic material is high than other transparent material. Similarity between the model and a full-sized object implies that the model can be used to predict the performance of the full sized object. Such a model is said to be mechanically similar to the full-sized object. Complete mechanical similarity requires geometric and dynamic similarity. Geometric similarity means that the model is true to scale in length, area, and volume. Dynamic similarity means that the ratios of all types of forces are equal. These forces result from inertia, gravity, viscosity, elasticity, surface tension, and pressure. Here we are considering the Reynolds dimensionless number. Reynolds number is ratio of inertia force to viscous force.

(Re) model = (Re) prototype

$$Re_m = \frac{\rho_m V_m L_m}{\mu_m} = \frac{\rho_p V_p L_p}{\mu_p} = Re_p \quad (11)$$

(Re) model = 18, 81,600 = (Re) prototype

Reynold number for prototype same kept as of model. Dimensions of prototype get reduced by 1/10th and velocity of prototype increased by 5 times than model. By giving scaled inlet boundary conditions to prototype Contour plot of scale down model appear same as of actual model and velocities of scale down model

increased by 5 times than actual. Because of the scalefactor, the use of full-scale installation velocities results in the ReynoldsNumber of the physical model being lower than that of its full-size counterpart. However, as long as the Reynolds number is high enough to insure that the flow is fully turbulent throughout the model.

J. Brian, P.E. Dumont, G. Robert, P.E. Mudry (2003), Computational Fluid Dynamic Modeling of Electrostatic Precipitators, *Electric Power 2003 Conference ICAC-EP-7 June 2004* Electrostatic Precipitator Gas Flow Model Studies
Fluent user guide

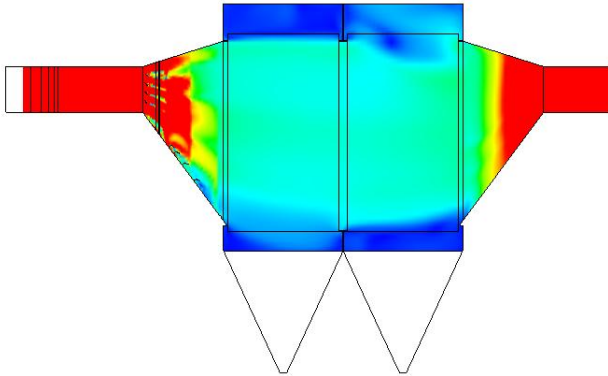


Fig.9 Scale down model contour plot.

6 Conclusion:

The effect of variable porosity of perforated plate on the flow distribution of ESP is discussed. By changing the porosity of perforated plate in the high velocity and low velocity region flow can be optimized. From table.3, it is seen that 90% number of points below 1.15 times V avg. and 100% number of points below 1.4 times V avg. and RMS within 20%. It shows flow is optimized. Scale down process is validate by comparing velocity contour of scale down with actual scale down contour ESP.

Reference

- Shah M. E. Haque, M. G. Rasul, M. M. K. Khan, A. V. Deev, and N. Subaschandar, (2007) Numerical modelling for optimizing flow distribution inside an electrostatic precipitator, *International journal of mathematics and computers in simulation, Issue 3, Volume 1*.
- Q. F. Hou^{1*}, B.Y. Guo L.F. Li and A. B. Yu Numerical simulation of gas flow in an electrostatic precipitator. *CSIRO December 2009 International Conference on CFD in the Minerals and Process Industries*
- B. Sahin and A. J. Ward-Smith, (1986), The use of perforated plates to control the flow emerging from a wide-angle diffuser, with application to electrostatic precipitator design, *Heat and Fluid Flow*, Vol 8, 124-131.
- Nikas, K.S.P., Varonos, A.A. and Bergeles, G.C., (2005), "Numerical simulation of the flow and the Collection mechanisms inside a laboratory scale Electrostatic precipitator". *J. Electrostatics*, 63, 423-443